Protein kinase involved in lung injury susceptibility: Evidence from enzyme isoform genetic knockout and *in vivo* inhibitor treatment

Mark S. Wainwright*, Janet Rossi*, James Schavocky†‡, Susan Crawford§, David Steinhorn*, Anastasia V. Velentza†‡, Magdalena Zasadzki†‡, Vladimir Shirinsky¶, Yuzhi Jia§, Jacques Haiech‖, Linda J. Van Eldik‡, and D. Martin Watterson†‡††**

Departments of *Pediatrics, †Molecular Pharmacology and Biological Chemistry, §Pathology, and **Cell and Molecular Biology, and the ‡Drug Discovery Program, Northwestern University, Chicago, IL 60611; ¶Laboratory of Cell Motility, Russian Cardiology Research Center, Moscow 121552, Russia; and ‖Institut G. Laustriat, Université Louis Pasteur and Centre National de la Recherche Scientifique Unité Mixte de Recherche 7034, F-67401 Illkirch, France

Communicated by David L. Garbers, University of Texas Southwestern Medical Center, Dallas, TX, March 19, 2003 (received for review January 29, 2003)

Acute lung injury (ALI) associated with sepsis and iatrogenic ventilator-induced lung injury resulting from mechanical ventilation are major medical problems with an unmet need for small molecule therapeutics. Prevailing hypotheses identify endothelial cell (EC) layer dysfunction as a cardinal event in the pathophysiology, with intracellular protein kinases as critical mediators of normal physiology and possible targets for drug discovery. The 210,000 molecular weight myosin light chain kinase (MLCK210, also called EC MLCK because of its abundance in EC) is hypothesized to be important for EC barrier function and might be a potential therapeutic target. To test these hypotheses directly, we made a selective MLCK210 knockout mouse that retains production of MLCK108 (also called smooth-muscle MLCK) from the same gene. The MLCK210 knockout mice are less susceptible to ALI induced by i.p. injection of the endotoxin lipopolysaccharide and show enhanced survival during subsequent mechanical ventilation. Using a complementary chemical biology approach, we developed a new class of small-molecule MLCK inhibitor based on the pharmacologically privileged aminopyridazine and found that a single i.p. injection of the inhibitor protected WT mice against ALI and death from mechanical ventilation complications. These convergent results from two independent approaches demonstrate a pivotal *in vivo* role for MLCK in susceptibility to lung injury and validate MLCK as a potential drug discovery target for lung injury.

Current hypotheses (1, 2) identify dysfunction of the endothelial cell (EC) layer as a cardinal event in the pathophysiology of multiple medical conditions, including sepsis. The mortality associated with sepsis alone is similar (3) to that of acute myocardial infarction (MI). In contrast to MI, available therapies are limited for the treatment of sepsis and its associated tissue injuries (3, 4). Mechanical ventilation is often required for the support of patients with sepsis but is itself associated with additional, iatrogenic pulmonary injury that also appears to involve EC barrier dysfunction (5). Recent progress in the use of controlled ventilator strategies, such as positive end-expiratory pressure (PEEP), lessens the potential for ventilator-induced lung injury (VILI), but a need still exists for therapies that would prevent this clinical complication (5). Most recently, *in vitro* studies have linked a variety of EC signal transduction pathways to the physiological mechanisms of EC barrier function and identified several endothelial protein kinases as potential drug discovery targets (1). However, the integration of the knowledge regarding *in vitro* signal transduction pathways with *in vivo* pathophysiology related to compromised EC barrier function and the validation of potential EC therapeutic targets have not occurred.

Homeostasis and resistance to tissue injury are maintained by a balance between intracellular EC cytoskeletal contraction–relaxation cycles and modulation of EC extracellular adhesion properties, which results in a regulated paracellular transport system, or barrier, that limits entry of activated leukocytes from the bloodstream into the tissue. In sepsis-related lung injury (6), it is the release of oxidative metabolites by penetrant leukocytes that causes lung tissue damage. *In vitro* studies (1) have implicated protein kinases such as myosin light-chain kinase (MLCK) and Rho kinase in the regulation of EC barrier function through their direct regulation of the phosphorylation state of myosin light chains and the intracellular cytoskeletal contraction–relaxation cycles. However, the *in vivo* role of such protein kinases in pathophysiology and their potential as drug discovery targets in diseases and injuries characterized by EC dysfunction, including acute lung injury (ALI) and VILI, are not known. *In vitro* studies with cells in culture (1) suggest the importance of the two myosin-regulating protein kinases in EC barrier function, but it is not clear how either kinase would be involved in the mechanism of response to an *in vivo* stress such as sepsis.

To determine the *in vivo* contribution of MLCK to acute tissue injuries such as ALI and VILI, we established an MLCK210 knockout (KO) mouse strain that retains production of MLCK108 from the same gene (MLKC108 refers to the computed mass of 108,000 for the ORF, although the protein migrates at an anomalously higher apparent molecular weight of ≈135,000 in SDS/PAGE.) Our results show that KO mice are less susceptible to endotoxin-induced ALI and the lethal complications associated with subsequent VILI. By using a complementary chemical biology approach, we developed a small-molecule MLCK inhibitor and found that a single i.p. injection of the inhibitor protected WT mice against lipopolysaccharide (LPS)-induced ALI and death from subsequent VILI. These convergent results from gene KO and chemical biology approaches provide a precedent in integrative biology, and a much needed animal model for future research in cardiovascular and pulmonary biology.

Materials and Methods

Animal Care. All procedures were performed in accordance with relevant National Institutes of Health guidelines and approved by the Institutional Animal Care and Use Committee of Northwestern University.

Construction and Characterization of MLCK210 KO Mouse. The genomic locus targeted in this study is that encoding the mouse MLCK210 and MLCK108, located on chromosome 16B4-B5 (7). This locus is different from the genomic locus encoding a protein of distinct amino acid sequence and tissue expression but also referred to as a MLCK, which is located on chromosome 2H1.

Abbreviations: ALI, acute lung injury; CaM, calmodulin; EC, endothelial cell; KO, knockout; LPS, lipopolysaccharide; MLCK, myosin light chain kinase; PEEP, positive end-expiratory pressure; VILI, ventilator-induced lung injury.

††To whom correspondence should be addressed. E-mail: m-watterson@northwestern.edu.

PHARMACOLOGY

A genomic clone containing a portion of the mouse MLCK210/108 locus was isolated from a 129/SvJ phage genomic library by a PCR screen with oligonucleotide primers 429F, 5′-GTCCTAGCATCTGGGGTGAG-3′, and 534R, 5′-CAGTGATCTTGCAGGAGAAT-3′, corresponding to exon 5 of EC MLCK. An ≈16-kb fragment mapped by subcloning, restriction enzyme digests, and Southern blotting contained the target exon 8. The targeting vector was constructed by blunt-end ligation of a 2.0-kb neomycin cassette into the *Sma*I site of exon 8 and inclusion of 2.5 kb of 5′ and 4.7 kb of 3′ flanking sequences from the MLCK210 gene.

Embryonic stem cells were electroporated with the linearized targeting construct and selected with G418. Homologous recombination in embryonic stem clones was assessed by Southern blot analysis by using *Eco*RI-digested genomic DNA hybridized with a 1.9-kb *Kpn*I–*Bam*HI probe (6.9 kb = WT; 7.7 kb = mutant allele). Embryonic stem clone 208 that was positive for the mutant allele was microinjected into a C57BL/6-derived blastocyst, which gave rise to a male with significant embryonic stem cell contribution as determined by Agouti coat color. Mating this founder male with C57BL/6 females and genotyping of offspring tail DNA by Southern hybridization confirmed germline transmission.

Genotypes from matings were done by Southern blot analysis as described above, which allows monitoring of both WT and mutant alleles. To demonstrate selective loss of the MLCK210 with retention of expression for MLCK108, homogenates of lung tissue were prepared, equivalent total protein amounts were loaded on SDS/PAGE, and gels were analyzed by Western blot with an anti-MLCK antibody (8) that recognizes both MLCK210 and MLCK108.

Injections and Ventilation of Mice. LPS (from *Salmonella typhimurium*; Sigma) was administered at a dose of 10 mg/kg i.p. injection. MLCK inhibitor (2.5 mg/kg) was administered to WT mice by i.p. injection just before treatment with LPS. Control mice received an equivalent volume of diluent. Two ventilator protocols were used. In the first protocol, mice were endotracheally intubated and ventilated under isoflurane anesthesia with a tidal volume (V_t) of 10–12 ml/kg by using a mouse ventilator (Harvard Bioscience, South Natick, MA). These studies were performed without application of PEEP. In the second set of studies, PEEP of 3 cm H_2O was applied during ventilation to reduce VILI. Core temperature was maintained at 36.5 ± 0.1°C by surface heating and cooling.

Analyses of Lung Injury. Paraffin-embedded hematoxylin/eosin-stained sections were prepared by standard techniques after perfusion with 4% paraformaldehyde. Sagittal sections through central and peripheral areas of each lobe were obtained to be representative of histological changes in the entire lung. A minimum of five fields at ×20 magnification were examined for each section. Quantal assessment of injury was performed in blinded fashion by grading four histological findings: hemorrhage, inflammation, atelectasis, and edema. Each feature was graded on a scale of 1 (normal) to 5 (diffuse abnormality). For each scale, the assignment of an injury score was based on the following criteria: (*i*) focal, multifocal, or contiguous lung involvement; and (*ii*) proximal or peripheral lung involvement. For the assessment of hemorrhage, inflammation, and edema, additional criteria evaluated included (*i*) the extravasation of fluid, red blood cells, or inflammatory cells, and (*ii*) the presence of polymorpho- or mononuclear cells. A composite lung-injury score was then calculated for each mouse on a scale from 4 (normal) to 20 (maximum injury) derived from the scores assessed for the four individual scales of histological injury. Samples for electron microscopy were prepared by using published protocols (9), and ultrasections contrasted with uranyl acetate and lead citrate. The water content of lungs of KO and WT mice was measured by calculating the wet/dry ratios. Mice were injected i.p. with saline or 10 mg/kg LPS and allowed to recover for 24 h. The lungs were then removed and weighed (wet weight) before drying for 72 h at 50°C (dry weight). Wet/dry weight ratio was calculated by dividing the wet weight by the dry weight.

Synthesis of MLCK Inhibitor. The chemical biology approach used to discover 11-(3-chloro-6-imino-6*H*-pyridazin-1-yl)-undecanoic acid (6-phenyl-pyridazin-3-yl)-amide was used previously (10–12) for protein kinase inhibitors on the basis of the pharmacologically privileged 3-aminopyridazine scaffold. Synthesis conditions and protocols have been described (11). In brief, alkylation of commercially available (Alfa Aesar, Ward Hill, MA) 3-amino-6-chloropyridazine resulted in the 11-(3-chloro-6-imino-6*H*-pyridazin-1-yl)-undecanoic acid ethyl ester, which was then hydrolyzed to the corresponding carboxylic acid. This product was coupled to the 3-amino-6-phenyl-pyridazine (10) by the 1-hydroxybenzotriazole hydrate/1-ethyl-3-(3-dimethylamino-propyl)carbodiimide method to yield the 11-(3-chloro-6-imino-6*H*-pyridazin-1-yl)-undecanoic acid (6-phenyl-pyridazin-3-yl)-amide. The reactions were monitored by analytical HPLC. The final product was purified by RP-HPLC chromatography on a preparative Microsorb (Rainin Instruments) C18 column with gradients of 0.1% (vol/vol) trifluoroacetic acid in water and 80% aqueous acetonitrile containing 0.08% trifluoroacetic acid. The final product was characterized by matrix-assisted laser desorption ionization–time-of-flight by using a PerSeptive Voyager-DE PRO system (Applied Biosystems). The experimentally determined mass (m/z) of 467.17 is in agreement with that expected (466.22) for the product ($C_{25}H_{31}ClN_6O$). Testing of compounds for kinase inhibitory activity against MLCK, the structurally and functionally related kinases death-associated protein kinase and calmodulin (CaM)-regulated protein kinase II, and the signal transduction pathway relevant kinases PKA and PKC was performed as described (10–13) by using the corresponding peptide substrates and assay conditions. Rho kinase and GSK3β assays were performed according to protocols provided by the manufacturer (Upstate Biotechnology, Lake Placid, NY). IC_{50} values were calculated by a linear regression analysis and kinetics determined as described (10–13). The MLCK inhibitor is competitive with the ATP substrate and has a K_i of ≈5 μM, similar in magnitude to the K_m value for the substrate. At concentrations up to 100 μM, the MLCK inhibitor did not inhibit death-associated protein kinase, a structurally similar CaM-regulated kinase that also uses myosin light chains as a protein substrate; CaM-regulated protein kinase II, a CaM-regulated kinase with broad tissue distribution and less stringent substrate specificity; GSK3β, another CaM kinase; or Rho kinase, a regulator of myosin light-chain phosphorylation through its phosphorylation of the myosin light-chain phosphatase. The concentrations of the inhibitor that fail to inhibit these relevant kinases are >20 times the K_i value of the inhibitor for MLCK, indicative of the inhibitor selectivity.

Statistical Analysis. Nonparametric lung-injury scores or wet/dry weights were compared between groups by the Mann–Whitney test or one-way analysis of variance (PRISM, GraphPad, San Diego) as appropriate. Lung-injury scores are reported as median and interquartile range. Differences in Kaplan–Meier survival curves were calculated by Mantel–Haenszel log rank test. Statistical significance was assumed when $P < 0.05$.

Results

Generation of MLCK210 KO Mouse Strain. We made a selective MLCK210 (EC MLCK) KO mouse, with retention of MLCK108 (SM MLCK) production from the same gene, by selective exon

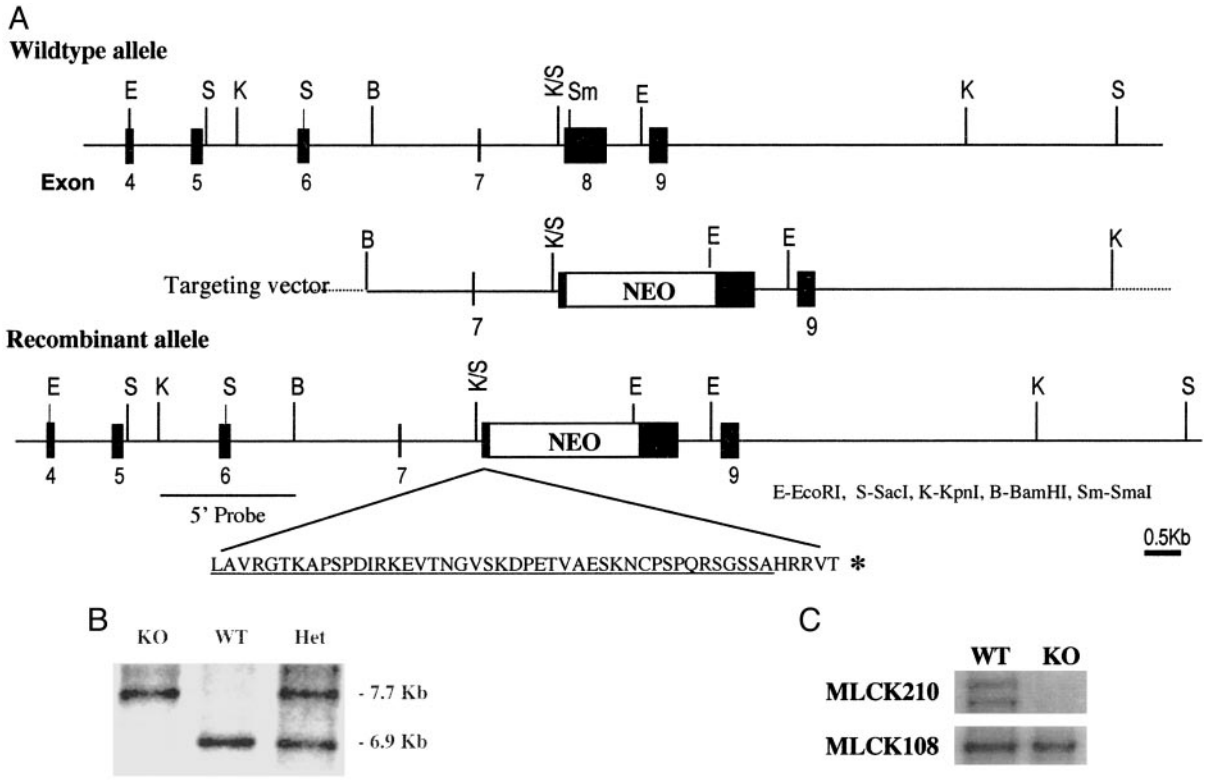

Fig. 1. MLCK210 KO mouse shows selective ablation of MLCK210 with retention of MLCK108 production. Shown are the targeting strategy and expression of gene products in the KO mouse. (*A*) Schematic representation of the mouse MLCK210 genomic organization around exons 4–9 and of the targeting vector. The targeting vector contains a neomycin (NEO) cassette inserted into the *Sma*I site of exon 8. The 1.9-kb *Kpn*I–*Bam*HI probe used for Southern blot analysis is shown. The underlined amino acid sequence represents the MLCK210 sequence upstream of the reading frame shift caused by the NEO cassette insertion. A stop codon (*) was inserted within the NEO cassette to ensure that MLCK210 translation was terminated. (*B*) Southern blot hybridization analysis of genotypes. The 6.9-kb band corresponds to the WT allele and the 7.7-kb band corresponds to the mutant allele. (*C*) Western blot analysis of lung tissue from KO and WT mice, with an anti-MLCK antibody that recognizes MLCK108 and all known splice variants of MLCK210.

targeting. We targeted a single exon (Fig. 1) that is specific for MLCK210 and upstream of the exons used by both MLCK108 and MLCK210 and of all known splice variants of MLCK210 and MLCK108. The introduction of multiple stop codons and a neomycin-resistance gene within the 1.8-kb DNA cassette (Fig. 1*A*) resulted in the disruption of the coding sequences in this exon without altering gene promoter activity and downstream splicing needed for MLCK108 production, allowed for antibiotic selection, and facilitated the detection of both the mutant and WT alleles by Southern blotting (Fig. 1*B*). The 6.9-kb band corresponds to the WT allele, and the 7.7-kb band corresponds to the mutant allele. Western blot analysis (Fig. 1*C*) of lung tissue homogenates from WT and homozygous KO mice reveals the loss of MLCK210. The levels of the MLCK108 produced from the same gene are preserved. The demonstration by protein Western blot that the MLCK210 is ablated but production of MLCK108 is retained and confirmatory Southern blot analysis of genomic DNA are indicative of gene disruption being localized within this narrowly restricted region of the gene. Gross pathology of KO mice revealed no dysmorphic features among organs, including lung, in young adults. No differences were found in litter size, weights, fertility, or viability between KO and WT mice strains.

ALI in MLCK210 KO Mice, WT Mice, and WT Mice Treated with MLCK Inhibitor. We administered by i.p. injection a bacterial endotoxin, LPS, as an initial, tractable surrogate for the systemic condition of sepsis. Histological examination of lung tissue from WT mice ($n = 13$) injected i.p. with LPS 24 h before sacrifice showed evidence of diffuse lung injury with intravascular and interstitial hemorrhage, inflammatory cell infiltrate, and atelectasis (Fig. 2*a*). In sharp contrast to the WT mice, the KO mice ($n = 7$) injected with LPS exhibited little evidence of injury (Fig. 2*b*). For example, the numerous thrombi occluding vessels and foci of RBC extravasation seen in the WT mice (Fig. 2*c*) were not seen in sections from the KO mice lungs (Fig. 2*d*). Similarly, multiple foci of leukocyte infiltration occurred in the WT mouse lung (Fig. 2*e*, arrow), which were not detected in the KO mice (Fig. 2*f*). These results are consistent with the preserved integrity of the endothelium in the KO lung. Quantal scoring (data expressed as median ± interquartile range) of the severity of histological lung injury (Fig. 2*g*) showed that the median lung-injury score was significantly higher ($P < 0.001$) in the WT mice (10 ± 5.5) than in the KO mice (6 ± 3.75), indicating that the KO mice were protected against the pulmonary injury associated with systemic exposure to endotoxin.

Pulmonary edema resulting from an abnormal extravasation of fluid is associated with EC barrier dysfunction during sepsis. Therefore, we used lung wet/dry weight changes to obtain an indication of potential differences in the effect of LPS treatment on the development of pulmonary edema in WT and KO mice. Analysis of lung wet/dry weight ratios (Fig. 2*h*) revealed that KO mice are less susceptible to LPS-induced pulmonary edema. Specifically, the wet/dry ratio (mean ± SEM) in control (saline-treated) WT mice was 4.5 ± 0.1 ($n = 6$), compared with 5.1 ± 0.2 in LPS-treated WT mice ($n = 7$; $P < 0.05$ compared with control). In the KO mice, the wet/dry ratio in control animals was 4.7 ± 0.3 ($n = 6$) compared with 4.5 ± 0.4 in LPS-treated

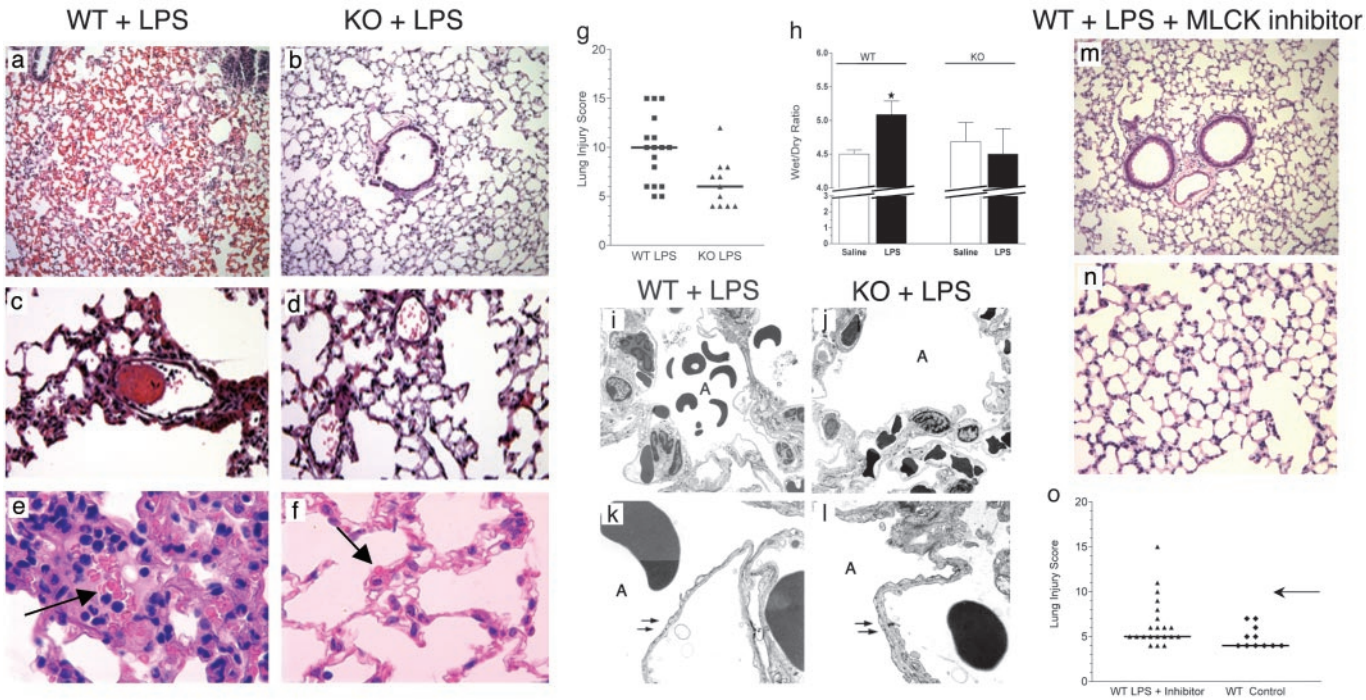

Fig. 2. Genetic KO or treatment with a MLCK inhibitor protects against ALI. (*a–f*) Hematoxylin/eosin staining of lung sections from WT (*a*, *c*, and *e*) and KO (*b*, *d*, and *f*) mice 24 h after i.p. injection of LPS (10 mg/kg). Arrows identify infiltrating leukocytes. (*g*) Quantal lung-injury scores of LPS-injected WT ($n = 13$) and KO ($n = 7$) mice. Each symbol reflects a separate slide, on which at least five fields from each lung section were scored in a blinded fashion. A horizontal line indicates the median lung-injury score. The KO mice show significantly lower ($P < 0.001$) lung-injury scores. (*h*) Lung wet/dry ratios (mean ± SEM) of WT mice injected with saline ($n = 6$) or LPS ($n = 7$) and KO mice injected with saline ($n = 6$) or LPS ($n = 6$). ⋆, Significantly different from saline-treated WT ($P < 0.05$). (*i–l*) Electron microscopy sections of lung prepared from WT (*i* and *k*) and KO (*j* and *l*) mice 24 h after LPS injection. A, alveolar space. Arrows identify endothelium. (*m* and *n*) Hematoxylin/eosin staining of lung sections from WT mouse 24 h after i.p. injection of LPS (10 mg/kg) and the MLCK inhibitor (2.5 mg/kg). (*o*) Lung-injury scores as in *g*, from WT mice injected with LPS + MLCK inhibitor ($n = 10$) or vehicle alone ($n = 6$). The arrow indicates the median score of WT mice injected with LPS alone (see *g*). Mice injected with LPS + inhibitor showed significantly lower ($P < 0.05$) lung-injury scores than WT mice injected with LPS alone. (Magnification: *a*, *b*, and *m*, ×10; *c*, *d*, and *n*, ×20; *e* and *f*, ×40; *i* and *j*, ×2,000; *k* and *l*, ×10,000.)

animals ($n = 6$). This difference between control KO mice and KO mice injected i.p. with LPS is not significant, suggesting that the KO mice exhibit preserved EC barrier function in response to endotoxin exposure.

Differential susceptibility of the WT and KO mice to damage of the EC layer after exposure to LPS is also indicated by electron microscopy results (Fig. 2 *i–l*). WT mice showed extravasation of RBCs across the EC barrier into the alveolar space (Fig. 2*i*), which was not observed in the KO mice (Fig. 2*j*). The endothelium of WT mice appeared thinner (Fig. 2*k*) than that of the KO mice (Fig. 2*l*). More detailed cell biological analyses and delineation of the molecular basis of the differences in electron microscopy appearance were not pursued as part of these initial characterizations of the KO mouse, but the results are congruent with the physiological and histological data that indicate a difference in endothelial layer function in the KO mice.

A single i.p. injection of the inhibitor, 11-(3-chloro-6-imino-6*H*-pyridazin-1-yl)-undecanoic acid (6-phenyl-pyridazin-3-yl)-amide, provided protection against endotoxin-induced lung injury to WT mice that is similar to that seen with the KO mice (compare Fig. 2 *m* and *b*). Specifically, we injected (i.p.) WT mice ($n = 10$) with 2.5 mg/kg of the MLCK inhibitor and LPS (10 mg/kg). Lung sections prepared from mice injected with LPS and the MLCK inhibitor were largely normal in appearance (Fig. 2 *m* and *n*). This level of protection is comparable to that seen in LPS-treated KO mice (Fig. 2*b*). Quantal scoring of the severity of histological lung injury (Fig. 2*o*) showed that the score of mice treated with LPS and MLCK inhibitor was significantly lower ($P < 0.001$; 5 ± 2.25) than mice treated with LPS alone (10 ± 5.5). WT mice treated with the MLCK inhibitor showed scores similar to those of control mice (4 ± 1.75).

Survival of Mice Subjected to VILI Subsequent to ALI. KO and WT mice subjected to LPS treatment that induced ALI (24 h after i.p. injection) were subjected to an experimentally tractable, surrogate treatment paradigm for VILI to probe differences in the complications of VILI after ALI. This was done by subjecting mice to endotracheal intubation and mechanical ventilation for a defined period in the absence of PEEP, conditions that represent an aggressive ventilation strategy. All of the WT mice treated with LPS ($n = 10$) died within 20 min of ventilation (Fig. 3). However, 67% of KO mice ($n = 6$) treated with LPS survived the full 60 min of ventilation, a dramatic difference in survival from the WT mice ($P < 0.001$ by log rank test). WT mice subjected to LPS treatment but also administered MLCK inhibitor were similarly protected from death as a result of VILI subsequent to ALI. Remarkably, 57% ($n = 7$) of WT mice treated with the MLCK inhibitor survived the full 60 min of mechanical ventilation. The survival of MLCK inhibitor-treated mice was significantly different from the survival of LPS-treated WT mice during ventilation ($P < 0.05$) and approximated the survival seen with the KO mice under the same conditions. Control mice, both KO and WT, that had not been injected with LPS tolerated the test period (60 min) of mechanical ventilation without difficulty (Fig. 3). Control mice injected with LPS but not ventilated also survived through the entire test period.

To determine whether the increase in survival during ventilation is simply a sequela of protection from LPS-induced ALI or also includes a VILI protection component, we examined the

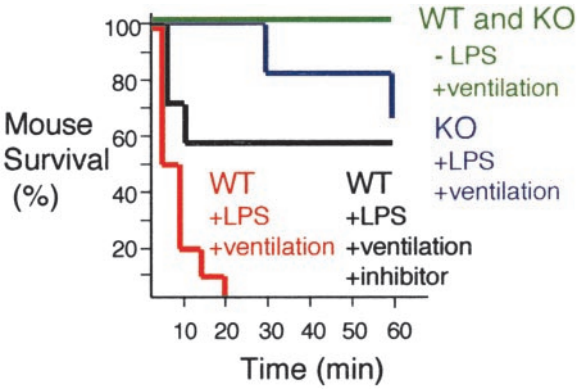

Fig. 3. Genetic KO or treatment with a MLCK inhibitor increases survival during mechanical ventilation after ALI. All WT mice ($n = 10$) injected i.p. with 10 mg/kg LPS 24 h earlier died within 20 min of ventilation. The majority (67%) of LPS-injected KO mice survived the 60-min test period of ventilation ($n = 6$). LPS-injected WT mice treated i.p. with 2.5 mg/kg MLCK inhibitor ($n = 7$) showed increased survival compared with WT mice exposed to LPS alone. Control WT and KO mice (not injected with LPS) survived 60 min of ventilation ($n = 4$). The difference in survival curves between LPS-treated WT and KO mice undergoing ventilation was significant ($P = 0.001$), as was the difference between LPS-treated WT mice undergoing ventilation with and without MLCK inhibitor ($P < 0.05$).

effects of applying PEEP during ventilation. If the increased mortality during ventilation of LPS-treated WT mice reflects a true VILI component, then PEEP should improve the survival of the WT mice. We found that all LPS-treated WT mice that had an applied PEEP of 3 cm H_2O to diminish VILI ($n = 9$) survived ventilation with PEEP support for 2 h, which is in contrast to 100% mortality within 20 min for LPS-treated WT mice ventilated in the absence of PEEP (Fig. 3). Analysis of VILI alone was not performed as part of this initial investigation. These initial results do not directly address the relative importance of MLCK in VILI, *per se*, and the experimental paradigm used here is not a model for the clinical syndrome. However, the results are indicative of MLCK210 involvement in susceptibility to ALI, as judged by histological criteria, and the complications of VILI subsequent to ALI, as judged by the physiological criteria of survival under injurious ventilation conditions.

Discussion

A principal finding of this investigation is the demonstration by both genetic KO and chemical biology approaches that inhibition of MLCK activity can protect against disease-relevant ALI, including complications associated with injury from mechanical ventilation, a widely used treatment in critical care medicine. The convergent results from two independent approaches, but common histological and physiological end points, demonstrate that MLCK plays an *in vivo* role in susceptibility to disease or injury, and provide a foundation for future drug discovery research in an area of unmet medical need.

The difference in susceptibility between KO and WT mice is consistent with the protection being due to maintenance of barrier function. The finding that a single treatment with a small-molecule inhibitor could approximate the histological protection and enhanced survival seen with MLCK210 gene KO is also consistent with protection of endothelial barrier function and the importance of MLCK-regulated cellular processes in injury from disease-related stresses. These *in vivo* protective effects are in agreement with *in vitro* studies (14, 15) of paracellular transport and the effects of MLCK activity increases. For example, increasing MLCK activity through the introduction of a constitutively active MLCK fragment into EC cultures results in hyperpermeability (14). The results, therefore, are consistent with a model in which stress-induced increases in MLCK activity result in hyperpermeability and altered barrier function, and decreased susceptibility from tissue injury is provided by the restoration of these processes back toward basal. Other MLCK-linked mechanisms of injury protection might also be involved, such as the restoration back toward normal of neutrophil adhesion, motility, and penetration of the EC layer (1, 15). The availability of the selective MLCK210 KO mouse strain will allow future *in vivo* studies of physiology related to EC barrier function that would not have been feasible in its absence. Further, the ablation in this KO mouse strain of the high molecular weight form of MLCK, but retention of the smooth muscle form of MLCK produced by the same gene, opens up new areas of *in vivo* vascular biology research, where previously the relative contribution of the two forms could not be determined readily.

The physiological effects of a gene KO of an enzyme, such as a protein kinase, do not necessarily reflect the function of the enzyme's catalytic activity. This finding is especially true when most of the protein mass is concerned with protein-docking interactions or scaffold functions, as seen with the noncatalytic domains of MLCK210 (16). The *in vivo* effects of the gene KO could reflect, instead, the effects on interacting or binding partners in the proteome. Further, a druggable molecular target (17) is one that can be modulated by an administered compound, so protection from disease-relevant insults by a gene KO model is just one step in target validation for drug discovery research. The essential requirement for target validation and mechanistic linkage to enzyme catalytic activity is the demonstration of inhibitor modulation of *in vivo* function. Therefore, we used our previously described (10–13) in-parallel, synthetic chemistry platform based on the pharmacologically privileged aminopyridazine structure (18, 19) to discover a small-molecule inhibitor of MLCK with high potential for *in vivo* use and examined its ability to mimic the protection seen with the targeted gene KO. The aminopyridazine scaffold has been used in drug development (18), so the cell-permeable and pharmacological properties of the inhibitor are consistent with its previous use in the discovery of bioavailable compounds. In terms of bioavailability properties, the MLCK inhibitor described here is rule-of-five compliant (20). The molecular weight is <500 ($= 467$), it has a calculated (ACD/LOGD SUITE, Version 5.11, Advanced Chemistry Development, Toronto) LogP <5 ($= 4.67 \pm 0.79$), the H-bond donors are <5 ($= 2$), and the H-bond acceptors are <10 ($= 5$). Consistent with these drug-like molecular properties, a single administration of the inhibitor at a tissue site (i.p.) remote from its site of action (lung) provided robust protection that partially mimics that seen with the gene KO. This remarkable precedent clearly raises the need for future drug discovery efforts to explore the potential use of aminopyridazine-based protein kinase inhibitors in conjunction with other therapies to minimize lung injury. It should be noted that the additional demand of oral availability may not be very relevant to this use because the clinically relevant mode of administration in such cases is usually injection or i.v. because of the compromised state of the patient. Therefore, the use of i.p. delivery in the studies described here is compatible with the intent-to-treat methodology that would be required in future investigations. Clearly, the particular inhibitor described here is not optimized and probably has other molecular interactions, especially at divergent doses, as is typical of first-generation small-molecule inhibitors. Therefore, it should not be considered a lead compound. However, the remarkable protection afforded by a single treatment with the inhibitor provides confirmation of the KO mouse results and suggests the potential for future development of similar small-molecule kinase inhibitors that are *in vivo* modulators of biological function. Taken in its entirety, the gene KO and chemical biology results indicate that intracellular protein kinase activity

is worthy of targeting in future drug discovery research in diseases involving endothelial barrier dysfunction.

The protection against tissue injury reported here raises the potential for targeting MLCK in drug discovery research for EC barrier injury, either as a primary target or cotreatment target. The endothelium is the primary vascular cell type in the pulmonary microvascular circulation, which is especially susceptible to injury in ALI and VILI. Therefore, the future development of compounds that would protect endothelium function is a challenge. The observation reported here that a small-molecule inhibitor administered at a remote site could mimic the lung protection seen with the MLCK210 gene KO suggests that the arduous task ahead may be worth consideration, especially considering the unmet need for therapies that differentially affect vascular beds. The ability of an intracellular signal transduction enzyme to serve as a drug discovery target is context-dependent, modulated by the upstream activating stimuli and the downstream transduction events. In this regard, CaM-regulated kinases are attractive targets. They function through a release-of-autoinhibition mechanism, which allows targeting of active sites that are fully accessible only in the transiently activated state brought about by upstream activating stimuli. A downstream signaling event that provides another level of filtering is MLCK's use of a single physiological substrate, myosin light chain. In addition, MLCK210 is less abundant in mammals than the smaller MLCK108, which is found at high levels in smooth muscle. This difference in kinase concentration allows the possibility of titrating, through therapeutic dosing, much of the MLCK210-derived activity, while retaining residual MLCK activity in the smooth muscle cell due to the more abundant MLCK108. It should be noted that the convergence of diverse signaling pathways on a single target, such as Rho kinase, and MLCK-mediated pathways converging on phosphorylation of myosin light chain, and the elaborate cross talk among pathways, which can provide redundancy and adaptive responses, require that structurally and functionally related kinases are not inhibited. The regulatory paradigm of intracellular signal transduction by protein phosphorylation makes the exhaustive *in vitro* testing of compounds against all known protein kinases a rather futile effort that can also generate misleading data. However, the rational testing of a set of functionally and structurally related kinases showed that the inhibitor described in this report does not inhibit Rho kinase or death-associated protein kinase, the latter being another CaM regulated protein kinase that also uses myosin light chain as a substrate. Clearly, molecular target selectivity and quantitative dosing of new compounds must be carefully addressed in future studies. However, the availability of the MLCK210-selective KO mouse and the potential for development of bioavailable inhibitors by using the privileged aminopyridazine chemical scaffold make the *in vivo* testing of such hypotheses more experimentally tractable.

We thank M. Mannix, C. Stephens, and Dr. L. Guo for their assistance. This study was supported in part by the Alzheimer's Association (D.M.W.), National Institutes of Health Grants RR13810 (to D.M.W.) and AG13939 (to L.J.V.E.), the Institute for the Study of Aging (D.M.W.), Howard Hughes Medical Institute Grant 55000335 (to V.S.), Russian Fund for Basic Research Grant 02-04-49341 (to V.S.), and the Women's Board of Children's Memorial Hospital, Chicago (M.S.W.). A.V.V. is a postdoctoral scholar in the Drug Discovery Training Program supported by National Institutes of Health Grant T32 AG00260.

1. van Hinsbergh, V. W. M. & van Nieuw Amerongen, G. P. (2002) *J. Anat.* **200,** 549–560.
2. National Institute of Neurological Disorders and Stroke (2002) *Report of the Stroke Progress Review Group* (Natl. Inst. of Neurol. Disorders and Stroke, Bethesda).
3. Angus, D. C., Linde-Zwirble, W. T., Lidicker, J., Clermont, G., Carcillo, J. & Pinsky, M. R. (2001) *Crit. Care Med.* **29,** 1303–1310.
4. Bernard, G. R., Vincent, J.-L., Laterre, P.-F., LaRosa, S. P., Dhainaut, J.-F., Lopez-Rodriguez, A., Steingrub, J. S., Garber, G. E., Helterbrand, J. D., Ely, E. W. & Fisher, C. J. (2001) *N. Engl. J. Med.* **344,** 699–709.
5. Tobin, M. (2001) *N. Engl. J. Med.* **344,** 1986–1996.
6. Stevens, T., Garcia, J., Shasby, D., Bhattacharya, J. & Malik, A. (2000) *Am. J. Physiol.* **279,** L419–L422.
7. Waterston, R. H., Lindblad-Toh, K., Birney, E., Rogers, J., Abril, J. F., Agarwal, P., Agarwala, R., Ainscough, R., Alexandersson, M., An, P., *et al.* (2002) *Nature* **420,** 520–562.
8. Watterson, D. M., Collinge, M., Lukas, T. J., Van Eldik, L. J., Birukov, K. G., Stepanova, O. V. & Shirinsky, V. P. (1995) *FEBS Lett.* **373,** 217–220.
9. Fan, C., Pan, J., Chu, R. Y., Lee, D., Kluckman, K. D., Usuda, N., Singh, I., Yeldandi, A. V., Rao, M. S., Maeda, N. & Reddy, J. K. (1996) *J. Biol. Chem.* **271,** 24698–24710.
10. Watterson, D. M., Mirzoeva, S., Guo, L., Whyte, A., Bourguignon, J.-J., Hibert, M., Haiech, J. & Van Eldik, L. J. (2001) *Neurochem. Int.* **39,** 459–468.
11. Mirzoeva, S., Sawkar, A., Zasadzki, M., Guo, L., Velentza, A., Dunlap, V., Bourguignon, J.-J., Ramstrom, H., Haiech, J., Van Eldik, L. J. & Watterson, D. M. (2002) *J. Med. Chem.* **45,** 563–566.
12. Velentza, A. V., Schumacher, A. M. & Watterson, D. M. (2002) *Pharmacol. Ther.* **93,** 217–224.
13. Velentza, A. V., Schumacher, A. M., Weiss, C., Egli, M. & Watterson, D. M. (2001) *J. Biol. Chem.* **276,** 38956–38965.
14. Tinsley, J., Lanerolle, P. D., Wilson, E., Ma, W. & Yuan, S. (2000) *Am. J. Physiol.* **279,** C1285–C1289.
15. Mamdouh, Z., Chen, X., Pierini, L. M., Maxfield, F. R. & Muller, W. A. (2003) *Nature* **421,** 748–753.
16. Kudryashov, D. S., Chibalina, M. V., Birukov, K. G., Lukas, T. J., Sellers, J. R., Van Eldik, L. J., Watterson, D. M. & Shirinsky, V. P. (1999) *FEBS Lett.* **463,** 67–71.
17. Hopkins, A. L. & Groom, C. R. (2002) *Nat. Rev. Drug Discov.* **1,** 727–730.
18. Wermuth, C. G. (1998) *J. Heterocycl. Chem.* **35,** 1091–1100.
19. Lipinski, C. A., Lombardo, F., Dominy, B. W. & Feeney, P. J. (2001) *Adv. Drug Deliv. Rev.* **46,** 3–26.
20. Patchett, A. A. & Nargund, R. P. (2000) *Annu. Rep. Med. Chem.* **35,** 289–298.